

CARLO BARONI <sup>1,2\*</sup>, MARTINA TENTI <sup>3</sup>, PHILIP J. BART <sup>4</sup>,  
MARIA CRISTINA SALVATORE <sup>1,2</sup>, Luca GASPERINI <sup>5</sup>, MARTINA Busetti <sup>6</sup>, CHIARA SAULI <sup>6</sup>,  
EUSEBIO MARIA STUCCHI <sup>1</sup> & ANDREA TOGNARELLI <sup>1</sup>

## ANTARCTIC ICE SHEET RE-ADVANCE DURING THE ANTARCTIC COLD REVERSAL IDENTIFIED IN THE WESTERN ROSS SEA *SUPPLEMENTARY MATERIAL*

### *Description of the layer stripping method*

Depth migration is a more complex processing step compared to time migration because it needs an accurate interval velocity field in depth. A way to understand whether the interval velocity field is accurate is the Migration Velocity Analysis (MVA), tool also available in the Promax environment, but manually carried out for this work. This procedure is performed with the layer stripping method, which is a methodology based on velocity field updating; in fact, it works determining an initial velocity value that must then be modified and updated layer by layer iteratively, starting from the most superficial reflector up to the deepest. The seafloor reflector is the first one to be horizontalized, usually using a velocity value equal to 1500 m/s (1470 m/s in this work) to update

the velocity field; if the horizon goes up, it means that the chosen velocity value was too low and needs to be increased, updating again the model; otherwise, if the horizon goes down, this means that the chosen velocity value was too high and must be decreased. Once seafloor reflector is flat, the same procedure must be repeated for the underneath reflector, keeping on until all the reflectors are flattened. Reflector flatness can be checked in the Common Image Gathers (CIGs).

Once velocity field has been updated, pre-stack depth migration must be run again by using the new velocity field. If the result is not good, all the steps can be performed again until reaching an acceptable model. Results are considered good when, displaying CIGs, all the reflectors are flattened and thus suitable to be stacked.

---

<sup>1</sup> Dipartimento di Scienze della Terra, University of Pisa, Via Santa Maria, 53, 56126 Pisa (PI), Italy.

<sup>2</sup> CNR-IGG, Istituto di Geoscienze e Georisorse, Pisa, Italy.

<sup>3</sup> Dipartimento di Scienze Ambientali, Informatica e Statistica, Università Cà Foscari di Venezia, Via Torino 155, 30172 Mestre (VE), Italy.

<sup>4</sup> Department of Geology and Geophysics, Louisiana State University, Baton Rouge, LA, USA.

<sup>5</sup> CNR-ISMAR, Istituto di Scienze Marine (Marine Geology), Bologna, Italy.

<sup>6</sup> Istituto Nazionale di Oceanografia e di Geofisica Sperimentale - OGS, Trieste, Italy.

\*Corresponding author: C. Baroni (carlo.baroni@unipi.it)

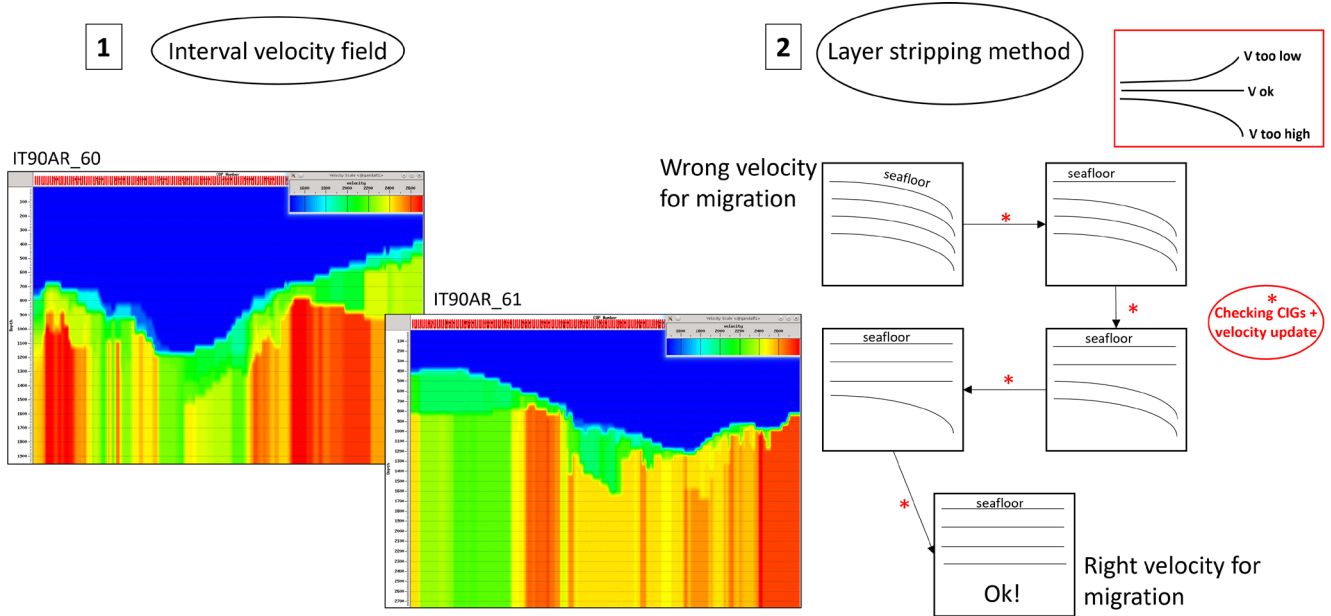


FIG. S1 - Migration velocity analysis. 1 = Interval velocity field in depth. 2 = Layer stripping method.

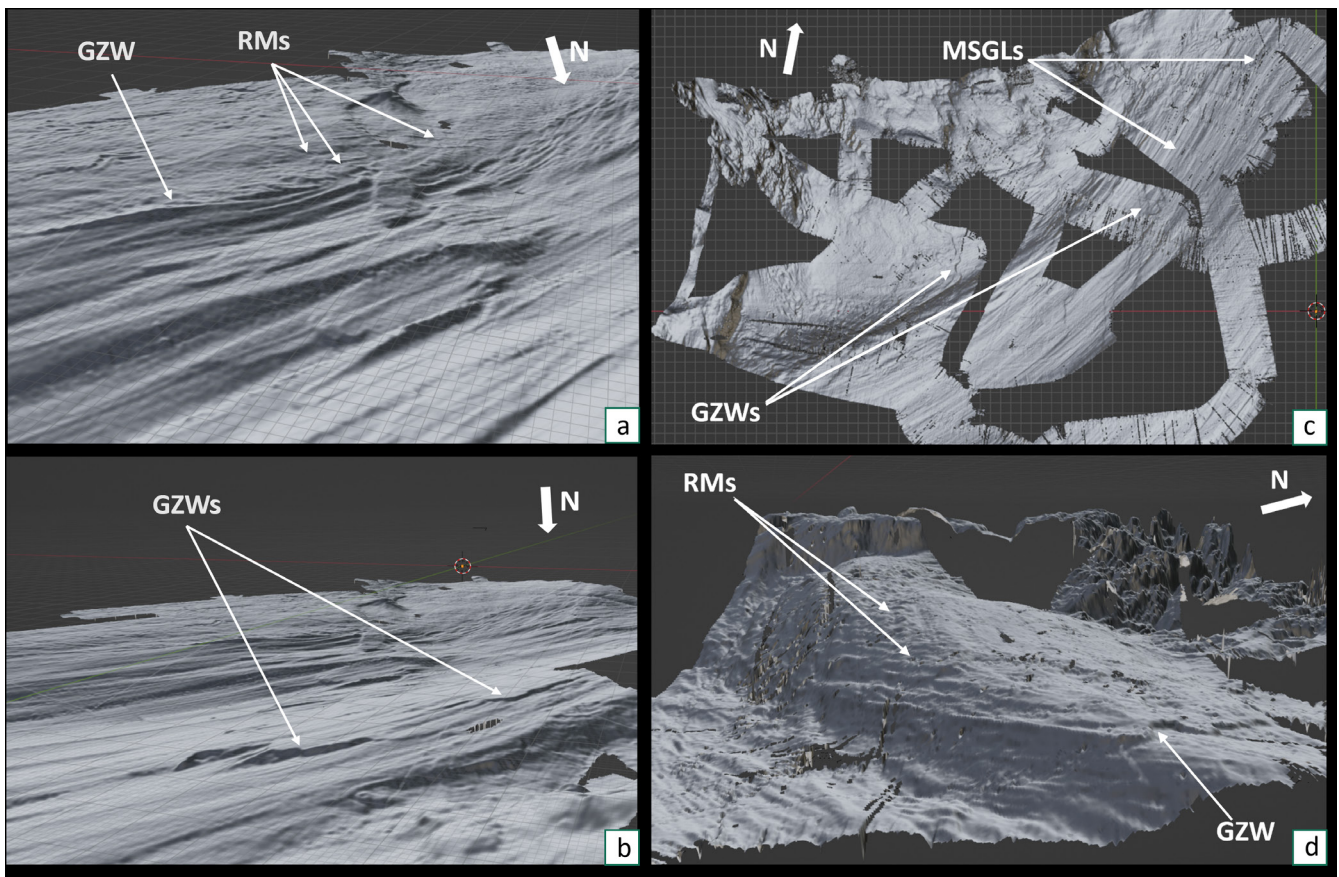


FIG. S2 - Construction of the 3D model starting from multibeam data in geotiff format. a) Detail of GZW detected on the eastern flank of Drygalski Basin and RMs on top of it. b) Two GZWs detected along the trough and testifying the post-LGM retreat. c) top view of US multibeam data related to NBP0801 cruise. d) Detail of GZW and RMs detected on the western flank of Drygalski Basin.

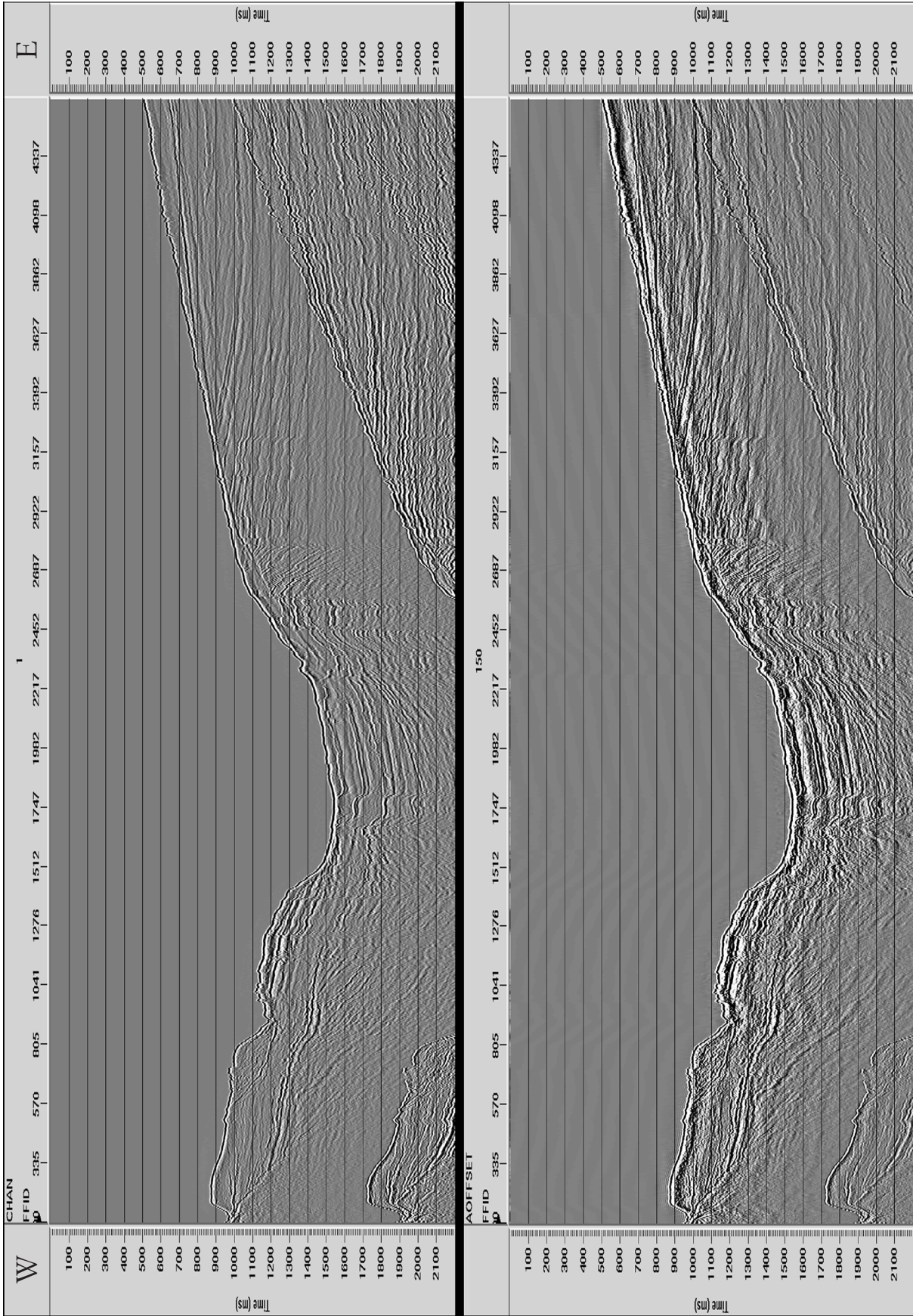


FIG. S3 - Seismic line IT90AR-60. Comparison between stacked data before (top) and after (bottom) predictive deconvolution.

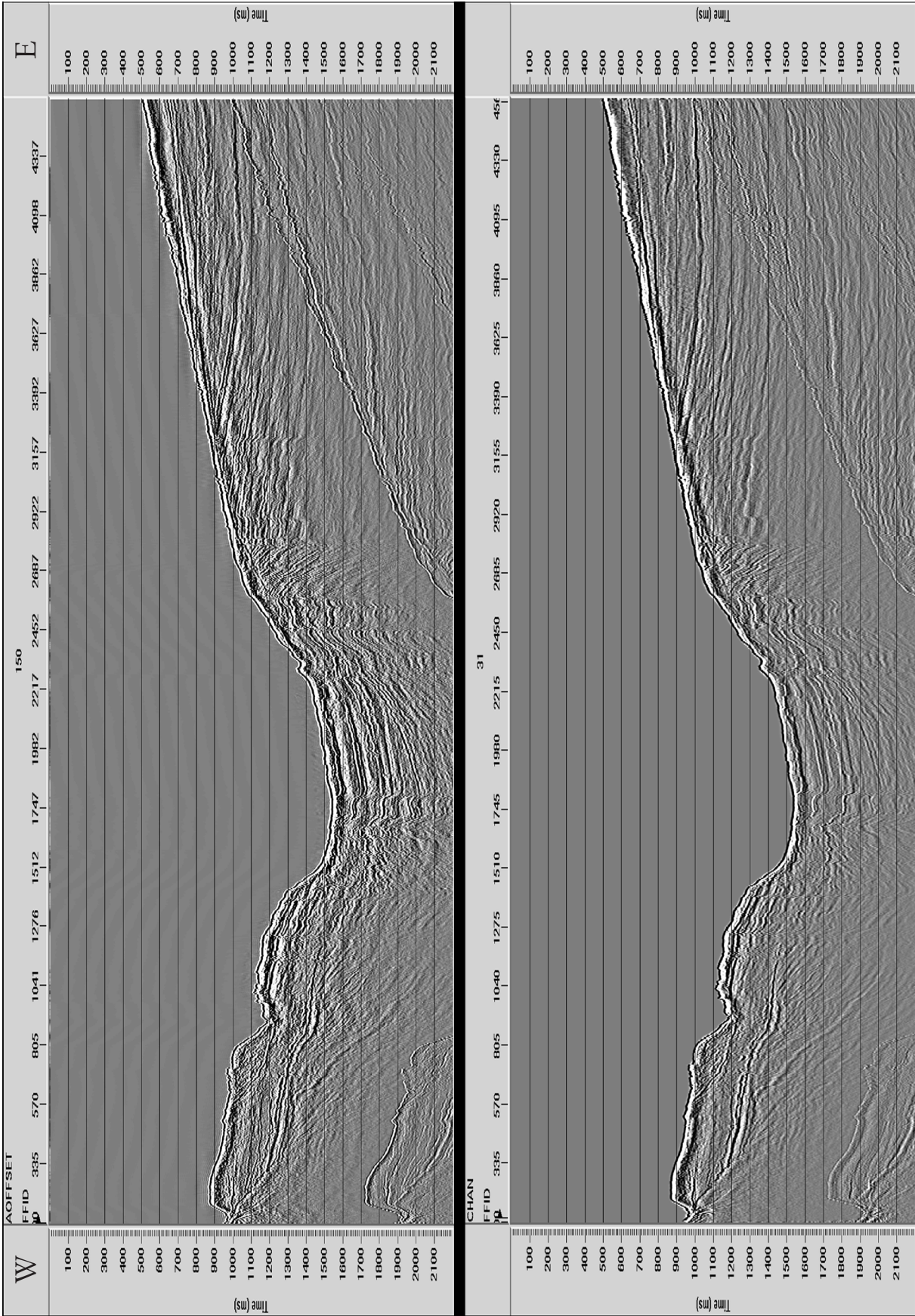


FIG. S4 - Seismic line IT90AR-60. Comparison between stacked data before (top) and after (bottom) the application of time migration.

TABLE S1 - Main acquisition parameters of the reprocessed seismic profiles IT90AR-60 and IT90AR-61.

Acquisition parameters	Values
Type of source	airguns
Total volume of airguns	22.5 l
Number of channels	120
Group interval	25 m
Shot interval	25 m
Sample interval	2 ms
Streamer length	2975 m
Recorder length	6 s
Min-Max offset	150-3125 m
Number of shots	4500 (IT60)-5127 (IT61)

TABLE S2 - Tests applied to trace autocorrelation and find the best parameters to apply to predictive deconvolution.  $\alpha$  = prediction lag; L = filter length.

IT90AR-60	$\alpha$	L
1	20	60
2	20	80
3	20	120
4	20	130
5	15	60
6	15	80
7	15	120
8	15	130
IT90AR-61	$\alpha$	L
1	15	60
2	15	130
3	15	280
4	20	180
5	20	280

TABLE S3 - List of dated sediment cores in the western Ross Sea (see fig. 8 for location of selected sites). Cores information from references, integrated with data from PNRA – Italian Antarctic Data Center (<https://iandc.pnra.aq/mna/search?keyword=Southern%20Pacific%20Ocean>) and from NOAA, National Centres for Environmental Information ([https://www.ncei.noaa.gov/maps/sample\\_index/](https://www.ncei.noaa.gov/maps/sample_index/), last access Dec.28, 2022).

cruise	corer type	core	LAT	LON	water depth (m)	core length (cm)	sample depth (cm)	material	age <sup>14</sup> C yr	lab code	St D	D <sup>13</sup> C	corrected age yr BP (from cited papers)	corrected age (-top age)	Correction method	cal age (median)	min cal age	max cal age	lithology	reference
ANTA02	gravity	AV43	-74.141	166.083	916	218	0-1	AIOM	1,878	AWI-4826.1.1	37	-22.7	modern	0	top	0	0	0	diatomaceous ooze	Di Roberto & alii, 2020
ANTA02	gravity	AV43	-74.141	166.083	916	218	130-131	AIOM	10,620	Poz-111,983	60	na	9,380	8,742	top	8,453	8,086	8,884	diatomaceous ooze	Di Roberto & alii, 2020
ANTA02	gravity 2,1 t	AV45	-74.207	165.799	648	339	3-4	AIOM	2,256	AWI-4827.1.1	38	-20.5	modern	0	top	0	0	0	diatomaceous ooze	Colizza & alii, 2004; Di Roberto & alii, 2020
ANTA02	gravity 2,1 t	AV45	-74.207	165.799	648	339	156-157	AIOM	9,460	GX-29994	50	-26.7	8260/8050	7,204	top	6881	6527	7235	diatomaceous ooze	Colizza & alii, 2004; Di Roberto & alii, 2020
ANTA91	gravity	14	-73.524	175.248	600	615	0-2	AIOM	5,420	OZB-931	50	na	1,620	0	top	0	0	0	mud	Frignani & alii, 1998
ANTA91	gravity	14	-73.524	175.248	600	615	259-261	AIOM	16,110	OZB-936	240	na	12,310	10,690	top	10,978	10,216	11,786	glacial marine sediments	Frignani & alii, 1998
ANTA91	gravity	14	-73.524	175.248	600	615	360-363	AIOM	25,090	OZB-938	860	na	21,290	19,670	top	22,053	20,026	23,980	glacial marine diamicton	Frignani & alii, 1998
ANTA91	gravity	19	-74.434	173.769	552	575	24-26	AIOM	4,470	na_1	70	na	3,240	1,470	3 ka	313	1	548	diatom/mud ooze	Salvi & alii, 2004
ANTA91	gravity	19	-74.434	173.769	552	575	206-209	AIOM	12,440	na_3	100	na	11,210	9,440	3 ka	9,316	8,857	9,781	sandy mud (transitional)	Salvi & alii, 2004
ANTA91	gravity	19	-74.434	173.769	552	575	376-382	foraminifers	19,020	na_4	100	na	17,790		carb	21,353	20,861	21,862	glacial marine diamicton	Salvi & alii, 2004
ANTA91	gravity	19	-74.434	173.769	552	575	570-575	foraminifers	30,380	na_5	600	na	29,150		carb	33,308	31,757	34,530	glacial marine diamicton	Salvi & alii, 2004
ANTA91	gravity	26	-74.182	168.498	700	237	0-2	AIOM	3,250	GX-23028	50	na	250	0	top	0	0	0	mud	Brambati & alii, 2002
ANTA91	gravity	26	-74.182	168.498	700	237	65-69	AIOM	18,650	GX-24302	140	na	15,650	15,400	top	17,080	16,539	17,647	glacial marine sediments	Brambati & alii, 2002
ANTA91	gravity	28	-74.394	167.127	975	191	0-2	AIOM	5,090	OZB-927	60	na	2,090	0	top	0	0	0	mud	Frignani & alii, 1998
ANTA91	gravity	28	-74.394	167.127	975	191	110-114	AIOM	17,490	OZB-930	930	na	14,490	12,400	top	13,187	10,757	15,623	glacial marine sediments	Frignani & alii, 1998
ANTA91	gravity	29	-75.109	164.219	1225	413	0-1	AIOM	6,710	OZB-922	50	na	3,710	0	top	0	0	0	mud	Frignani & alii, 1998
ANTA91	gravity	29	-75.109	164.219	1225	413	239-241	AIOM	17,370	OZB-925	90	na	14,370	10,660	top	10,930	10,430	11,394	glacial marine sediments	Frignani & alii, 1998
ANTA91	gravity	29	-75.109	164.219	1225	413	249-251	AIOM	28,090	OZB-926	290	na	25,090	21,380	top	24,001	23,216	24,795	subglacial diamicton	Frignani & alii, 1998
ANTA91	gravity	30	-74.951	165.783	1112	310	0-2	AIOM	4,935	GrA-987	35	na	3,535	0	top	0	0	0	siliceous mud	Brambati & alii, 1997
ANTA91	gravity	30	-74.951	165.783	1112	310	22-24	AIOM	11,365	GrA-985	45	na	9,965	6,430	top	6,035	5,683	6,362	laminated clayey silt	Brambati & alii, 1997
ANTA91	gravity	30	-74.951	165.783	1112	310	71.5-74	AIOM	16,950	GrA-986	60	na	15,550	12,015	top	12,755	12,458	13,075	silty clay	Brambati & alii, 1997
ANTA96	gravity	8	-75.267	171.199	583	174	35-37	AIOM	17,330	GX-24300	120	na	13,530	14,330	3 ka	18,944	18,533	19,442	glacial marine diamicton	Finocchiaro & alii, 2000; Melis & Salvi, 2009
ANTA96	gravity	8	-75.267	171.199	583	174	51.5-54	AIOM	24,830	GX-25712	110	na	21,030	21,830	3 ka	27,293	26,961	27,649	subglacial diamicton	Finocchiaro & alii, 2000; Melis & Salvi, 2009
ANTA96	gravity	9	-75.148	172.982	562	254	156-158	AIOM	10,100	GX-20301	60	na	6,300	7,100	3 ka	6,763	6,407	7,139	glacial marine diamicton	Finocchiaro & alii, 2000; Melis & Salvi, 2009
ANTA99	gravity	cD38	-75.700	165.300	800	295	162-163	AIOM	12,270	GX-30079	20	na	9,270	9,270	3 ka	9,122	8,722	9,466	clayey silt/silty clay	Finocchiaro & alii, 2007
ANTA99	gravity	cD38	-75.700	165.300	800	296	283-283.5	AIOM	28,070	GX-31330	300	na	25,070	25,070	3 ka	27,794	27,185	28,522	clayey silt/silty clay	Finocchiaro & alii, 2007
ANTA99	gravity	cD38	-75.700	165.300	800	297	227-228	AIOM	29,550	GX-30080	240	na	26,550	26,550	3 ka	29,330	28,759	29,900	sandy silt/silty sand	Finocchiaro & alii, 2007
ANTA99	gravity	J5	-73.494	175.390	598	553	5-6	AIOM	5,000	GX-27619	30	-30.6	1,200	2,000	3 ka	789	513	1,084	diatom mud / ooze	Salvi & alii, 2004
ANTA99	gravity	J5	-73.494	175.390	598	553	59-60	AIOM	6,120	GX-28117	40	-30.6	2,320	3,120	3 ka	1,999	1,612	2,355	diatom mud / ooze	Salvi & alii, 2004
ANTA99	gravity	J5	-73.494	175.390	598	553	139-140	AIOM	8,620	GX-28118	40	-29.5	4,820	5,620	3 ka	5,131	4,780	5,507	diatom mud / ooze	Salvi & alii, 2004
ANTA99	gravity	J5	-73.494	175.390	598	553	240-241	AIOM	13,850	GX-28116	50	na	10,050	10,850	3 ka	11,211	10,747	11,681	sandy mud (transitional glacial marine sediment)	Salvi & alii, 2004
ANTA99	gravity	J5	-73.494	175.390	598	553	397-398	AIOM	33,010	GX-30078	280	na	29,210	30,010	3 ka	32,942	31,990	33,750	sandy mud (glacial diamicton)	Melis & Salvi., 2009
ANTA99	gravity	NW27	-72.597	172.055	524	327	71-72	AIOM	27,640	GX-28119	260	na	24,640	24,640	3 ka	27,385	26,807	27,965	silty sand with pebbles	Melis & alii, 2002
ANTA99	gravity	NW27	-72.597	172.055	524	327	231-232	AIOM	31,560	GX-28120	400	na	28,560	28,560	3 ka	31,226	30,304	32,139	glacial marine sediment	Colizza & alii, 2003
ANTA99	gravity	NW31	-73.135	170.593	535	372	41-42	AIOM	8,800	GX-28121	50	na	5,800	5,800	3 ka	5,346	4,947	5,693	biogenic mud	Melis & alii, 2002
ANTA99	gravity	NW31	-73.135	170.593	535	372	91-92	AIOM	25,290	GX-28122	190	na	22,290	22,290	3 ka	25,045	24,457	25,621	silty clay (glac. marine sed.)	Melis & alii, 2002
ANTA99	gravity	NW31	-73.135	170.593	535	372	217-218	AIOM	30,380	GX-28123	340	na	27,380	27,380	3 ka	30,148	29,369	30,876	glacial marine diamicton	Colizza & alii, 2003
BAY05	box core	BC40	-74.183	166.050	1033	-	0.5	AIOM	2,230	OS-90283	30	-24.24	930			modern	modern	modern	faintly laminated ooze	Mezgec & alii, 2017
DF80	piston core	PC102	-75.200	163.717	1116	130	0-7	AIOM	4,025	AA-13244	55	na	2,825	1,025	3 ka	0	0	0	mud	Licht & alii, 1996
DF80	piston core	PC102	-75.200	163.717	1116	130	90	AIOM	12,640	CAMS-12581	80	na	11,440	9,640	3 ka	9,578	9,152	10,049	mud	Licht & alii, 1996
DF80	piston core	PC108	-75.067	166.000	915	171	22-26	AIOM	11,545	AA-13242	95	na	10,345	8,545	3 ka	8,227	7,844	8,614	mud	Licht & alii, 1996
DF80	piston core	PC111	-74.917	167.483	554	120	10-12	AIOM	4,750	CAMS-8253	70	na	3,550	1,750	3 ka	564	271	881	mud	Licht & alii, 1996
DF80	piston core	PC112	-74.917	166.817	713	135	5-6.5	AIOM	5,390	CAMS-4061	70	na	4,190	2,390	3 ka	1,172	830	1,518	mud	Licht & alii, 1996
DF80	piston core	PC132	-75.550	166.133	668	230	45-47	AIOM	8,390	CAMS-8251	80	na	7,190	5,390	3 ka	4,851	4,427	5,279	mud	Licht & alii, 1996
DF80	piston core	PC132	-75.550	166.133	668	230	62-65	AIOM	10,730	CAMS-11793	80	na	9,530	7,730	3 ka	7,421	7,078	7,751	mud	Licht & alii, 1996
DF80	piston core	PC144	-73.017	172.167	457	219	8-11	Alcyonarian coral	895	AA-11877	50	na	modern	modern		modern	modern	modern	muddy sand	Licht & alii, 1996
DF80	piston core	PC144	-73.017	172.167	457	219	8-11	AIOM	6,330	CAMS-11798	80	na	5,130	6,030	3 ka	5,604	5,239	5,984	muddy sand	Licht & alii, 1996
DF80	piston core	PC144	-73.017	172.167	457	219	10	Globo. Subglobosa	12,890	AA-17398	105	na	11,690		carb	12,393	11,885	12,757	muddy sand	Licht & alii, 1996

cruise	corer type	core	LAT	LON	water depth (m)	core length (cm)	sample depth (cm)	material	age <sup>14</sup> C yr	lab code	St D	D <sup>13</sup> C	corrected age yr BP (from cited papers)	corrected age (-top age)	Correction method	cal age (median)	min cal age	max cal age	lithology	reference
DF80	piston core	PC144	-73.017	172.167	457	219	13-14	foraminifers	21,255	AA-12899	200	na	20,055		carb	22,544	22,005	23,052	glacial marine diamicton	Licht & alii, 1996
DF80	piston core	PC144	-73.017	172.167	457	219	21-24	AIOM	22,360	CAMS-12582	140	na	21,160	19,360	3 ka	21,778	21,228	22,271	glacial marine diamicton	Licht & alii, 1996
DF80	piston core	PC144	-73.017	172.167	457	219	200	Globo. Subglobosa	32,685	CAMS-7790	610	na	31,485	31,485	carb	34,525	33,235	35,795	glacial marine diamicton	Licht & alii, 1996
DF80	piston core	PC177	-73.683	171.817	529	281	0-3	AIOM	7,470	CAMS-7790	70	na	6,270	0	top	0	0	0	sandy mud	Licht & alii, 1996
DF80	piston core	PC177	-73.683	171.817	529	281	30	benthic foraminifers	24,835	AA-15699	240	na	23,635		carb	26,405	25,840	27,010	glacial marine diamicton	Licht & alii, 1996
DF80	piston core	PC177	-73.683	171.817	529	281	230-233	foraminifers	27,255	AA-11878	305	na	26,055		carb	28,800	28,000	29,574	glacial marine diamicton	Licht & alii, 1996
DF80	piston core	PC177	-73.683	171.817	529	281	270	benthic foraminifers	30,170	AA-13229	475	na	28,970		carb	31,683	30,754	32,986	glacial marine diamicton	Licht & alii, 1996
DF87	piston core	PC20	-72.538	174.970	622	85	8-13	carbonates	27,590	na_6	460	na			carb	30,331	29,341	31,132	thick. gravelly calcareous sand	Taviani & alii, 1993
DF87	piston core	PC20	-72.538	174.970	622	85	34-40	carbonates	>35750	na_7	-	na			carb	>35750	>35751	>35752	thick. gravelly calcareous sand	Taviani & alii, 1993
DF87	piston core	PC32	-73.49	170.39	457	189	18-20	AIOM	23,390	CAMS-4062	240	na	22,190	20,390	3 ka	22,893	22,303	23,600	mud	Licht & alii, 1996
DF87	piston core	PC32	-73.49	170.39	457	189	80-84.5	mixed shells	27,720	AA-9361	340	na	26,520		carb	30,453	29,813	31,085	mud	Licht & alii, 1996
DF87	piston core	PC32	-73.49	170.39	457	189	119-121	AIOM	19,400	CAMS-4063	310	na	18,200	16,400	3 ka	18,257	17,403	18,988	mud	Licht & alii, 1996
ELT52	piston core	PC9	-72.447	173.872	479	471	10-12	carbonates	22,730	na_10	900	na			carb	25,431	23,557	27,263	coarse. bioclastic gravelly sands and muds	Taviani & alii, 1993
NBP15-02	karsten core	KC44	-75.660	166.810	486	125	64-66	AIOM	7,258	na_11	56	na	6,490	4,258	3 ka	3,393	2,999	3,801	diatomaceous sediment	Yokoyama & alii, 2016
NBP15-02	karsten core	KC44	-75.660	166.810	486	125	99-100	AIOM	27,579	na_12	150	na	29,975	24,579	3 ka	27,336	26,964	27,711	subglacial till	Yokoyama & alii, 2016, Halberstadt & alii, 2018
NBP94-01	piston core	PC17	-74.490	173.801	556	366	4-6	AIOM	9,690	AA-13942	70	na	6,690	6,690	3 ka	6,314	5,939	6,665	marine sediments	Domack & alii, 1999
NBP94-01	piston core	PC17	-74.490	173.801	556	366	10-12	AIOM	30,210	AA-13943	410	na	27,210	27,210	3 ka	29,964	29,106	30,824	subglacial till	Domack & alii, 1999
NBP94-01	trigger (gravity) core	TC16	-74.652	174.570	465	82	0-1	AIOM	4,410	AA-13970	50	na	0	0	top	0	0	0	gray diatomaceous mud and ooze	Domack & alii, 1999
NBP94-01	trigger (gravity) core	TC16	-74.652	174.570	465	82	15-16	AIOM	11,660	AA-13971	90	na	7,250	7,250	top	6,930	6,538	7,303	gray diatomaceous mud and ooze	Domack & alii, 1999
NBP94-01	trigger (gravity) core	TC16	-74.652	174.570	465	82	30-31	AIOM	13,380	AA-13972	85	na	8,970	8,970	top	8,733	8,332	9,175	granulated facies	Domack & alii, 1999
NBP94-01	trigger (gravity) core	TC16	-74.652	174.570	465	82	45-46	AIOM	18,010	AA-13973	125	na	13,600	13,600	top	14,676	14,057	15,241	diamicton	Domack & alii, 1999
NBP94-01	trigger (gravity) core	TC16	-74.652	174.570	465	82	53-55	AIOM	32,520	AA-13974	475	na	28,110	28,110	top	30,777	29,889	31,707	diamicton	Domack & alii, 1999
NBP94-01	trigger (gravity) core	TC17	-74.490	173.801	556	48	0-2	AIOM	3,340	AA-13944	45	na	0	0	top	0	0	0		Domack & alii, 1999
NBP94-01	trigger (gravity) core	TC17	-74.490	173.801	556	48	14-16	AIOM	4,480	AA-13945	50	na	1,140	1,140	top					Domack & alii, 1999
NBP94-01	trigger (gravity) core	TC17	-74.490	173.801	556	48	24-26	AIOM	5,170	AA-13946	50	na	1,830	1,830	top	634	345	925		Domack & alii, 1999
NBP94-01	trigger (gravity) core	TC17	-74.490	173.801	556	48	34-36	AIOM	5,700	AA-13947	50	na	2,360	2,360	top	1,142	811	1,466		Domack & alii, 1999
NBP94-01	trigger (gravity) core	TC17	-74.490	173.801	556	48	44-46	AIOM	6,510	AA-13948	45	na	3,170	3,170	top	2,061	1,684	2,452		Domack & alii, 1999
NBP94-01	trigger (gravity) core	TC18	-74.383	173.304	560	53	0-2	AIOM	4,440	AA-13949	60	na	0	0	top	0	0	0	gray diatomaceous mud and ooze	Domack & alii, 1999
NBP94-01	trigger (gravity) core	TC18	-74.383	173.304	560	54	14-16	AIOM	11,320	AA-13950	80	na	6,880	6,880	top	6,519	6,166	6,912	gray diatomaceous mud and ooze	Domack & alii, 1999
NBP94-01	trigger (gravity) core	TC18	-74.383	173.304	560	55	26-27	AIOM	14,620	AA-13951	100	na	10,180	10,180	top	10,285	9,745	10,772	brown diatomaceous mud and ooze	Domack & alii, 1999
NBP94-01	trigger (gravity) core	TC18	-74.383	173.304	560	56	37-39	AIOM	20,020	AA-13952	230	na	15,580	15,580	top	17,307	16,625	18,000	gravel and sand layer	Domack & alii, 1999
NBP94-01	trigger (gravity) core	TC20	-74.292	172.863	513	77	0-2	AIOM	3,580	AA-13961	50	na	0	0	top	0	0	0		Domack & alii, 1999
NBP94-01	trigger (gravity) core	TC20	-74.292	172.863	513	77	11-12	AIOM	5,980	AA-13962	60	na	2,400	2,400	top	1,182	852	1,523		Domack & alii, 1999
NBP94-01	trigger (gravity) core	TC20	-74.292	172.863	513	77	25-26	AIOM	8,950	AA-13963	70	na	5,370	5,370	top	4,824	4,418	5,256		Domack & alii, 1999
NBP94-01	trigger (gravity) core	TC20	-74.292	172.863	513	77	38-40	AIOM	13,120	AA-13964	90	na	9,540	9,540	top	9,443	9,002	9,900		Domack & alii, 1999
NBP94-01	trigger (gravity) core	TC20	-74.292	172.863	513	77	45-47	AIOM	18,370	AA-13965	140	na	14,790	14,790	top	16,319	15,776	16,871		Domack & alii, 1999
NBP95-01	surface grab sample	G54	-73.150	174.968	381	-	0	Bathylasma sp.	1,090	AA-17374	45	0.8	modern		top	#N/D	#N/D	#N/D		Domack & alii, 1999
NBP95-01	surface grab sample	G54	-73.150	174.968	381	-	0	Bathylasma sp.	1,130	AA-17375	45	1	modern		top	#N/D	#N/D	#N/D		Domack & alii, 1999
NBP95-01	kasten core	KC31	-75.700	165.417	879	225	0-2	AIOM	2,424	AA-17364	50	na	0	0	top	0	0	0	massive mud	Cunningham & alii, 1999
NBP95-01	kasten core	KC31	-75.700	165.417	879	225	0-2	AIOM	2,430	AA-17364	50	-23.7		0	top	0	0	0	diatom mud and ooze	Domack & alii, 1999
NBP95-01	kasten core	KC31	-75.700	165.417	879	225	9-11	AIOM	3,140	AA-17365	50	na	715	716	top	#N/D	#N/D	#N/D	massive mud	Cunningham & alii, 1999
NBP95-01	kasten core	KC31	-75.700	165.417	879	225	9-11	AIOM	3,140	AA-17365	50	-24.8		710	top	#N/D	#N/D	#N/D	diatom mud and ooze	Domack & alii, 1999
NBP95-01	kasten core	KC31	-75.700	165.417	879	225	30-32	AIOM	3,940	AA-21766	45	na	1,515	1,516	top	353	53	618	massive mud	Cunningham & alii, 1999
NBP95-01	kasten core	KC31	-75.700	165.417	879	225	49-51	AIOM	5,680	AA-17366	55	na	3,255	3,256	top	2,160	1,763	2,576	massive mud	Cunningham & alii, 1999
NBP95-01	kasten core	KC31	-75.700	165.417	879	225	49-51	AIOM	5,680	AA-17366	55	-24.8		3,250	top	2160	1763	2576	diatom mud and ooze	Domack & alii, 1999
NBP95-01	kasten core	KC31	-75.700	165.417	879	225	70-72	AIOM	5,925	AA-21767	60	na	3,500	3,501	top	2,476	2,076	2,843	massive mud	Cunningham & alii, 1999
NBP95-01	kasten core	KC31	-75.700	165.417	879	225	87-89	AIOM	7,270	AA-21768	65	na	4,845	4,846	top	4,145	3,710	4,564	massive mud	Cunningham & alii, 1999
NBP95-01	kasten core	KC31	-75.700	165.417	879	225	116-118	AIOM	10,230	AA-17367	70	na	7,805	7,806	top	7,487	7,166	7,805	mud with sandy layers	Cunningham & alii, 1999
NBP95-01	kasten core	KC31	-75.700	165.417	879	225	116-118	AIOM	10,230	AA-17367	70	-27.7		7,800	top	7487	7166	7805	gray mud	Domack & alii, 1999
NBP95-01	kasten core	KC31	-75.700	165.417	879	225	159-161	AIOM	12,275	AA-17368	95	na	9,850	9,851	top	9,838	9,413	10,260	pebbly. massive diamicton	Cunningham & alii, 1999
NBP95-01	kasten core	KC31	-75.700	165.417	879	225	159-161	AIOM	12,280	AA-17368	95	-26.9	11,270	9,850	top	9,838	9,413	10,260	muddy gravel with till granules	Domack & alii, 1999

cruise	corer type	core	LAT	LON	water depth (m)	core length (cm)	sample depth (cm)	material	age <sup>14</sup> C yr	lab code	St D	D <sup>13</sup> C	corrected age yr BP (from cited papers)	corrected age (-top age)	Correction method	cal age (median)	min cal age	max cal age	lithology	reference
NBP95-01	kasten core	KC31	-75.700	165.417	879	225	167-169	AIOM	26,265	AA-20743	325	na	23,840	23,841	top	26,604	25,884	27,261	pebbly. massive diamicton	Cunningham & alii, 1999
NBP95-01	kasten core	KC31	-75.700	165.417	879	225	200	AIOM	31,605	AA-20744	520	na	29,225	29,181	top	31,947	30,871	33,271	pebbly. massive diamicton	Cunningham & alii, 1999
NBP95-01	kasten core	KC34	-75.165	164.494	1257	245	0.1	AIOM	3,205	AA-20745	60	-24.7	1,905		top	#N/D	#N/D	#N/D		Andrews & alii, 1999
NBP95-01	kasten core	KC37	-74.498	167.743	924	175	0-2	AIOM	2,775	AA-17357	50	na	0	0	top	0	0	0	massive mud	Cunningham & alii, 1999
NBP95-01	kasten core	KC37	-74.498	167.743	924	175	0-2	AIOM	2,780	AA-17357	50	-24.4		0	top	0	0	0	diatom mud and ooze	Domack & alii, 1999
NBP95-01	kasten core	KC37	-74.498	167.743	924	175	10-11	AIOM	3,020	AA-17363	50	na	245	245	top	#N/D	#N/D	#N/D	massive mud	Cunningham & alii, 1999
NBP95-01	kasten core	KC37	-74.498	167.743	924	175	10-11	AIOM	3,020	AA-17363	50	-24.8		240	top	#N/D	#N/D	#N/D	diatom mud and ooze	Domack & alii, 1999
NBP95-01	kasten core	KC37	-74.498	167.743	924	175	20-21	AIOM	4,715	AA-17358	50	na	1,940	1,940	top	735	468	1,045	massive mud	Cunningham & alii, 1999
NBP95-01	kasten core	KC37	-74.498	167.743	924	175	20-21	AIOM	4,720	AA-17358	50	-25.3		1,940	top	735	468	1045	diatom mud and ooze	Domack & alii, 1999
NBP95-01	kasten core	KC37	-74.498	167.743	924	175	30-31	AIOM	6,205	AA-17362	55	na	3,430	3,430	top	2,392	1,993	2,748	massive mud	Cunningham & alii, 1999
NBP95-01	kasten core	KC37	-74.498	167.743	924	175	30-31	AIOM	6,210	AA-17362	55	-25.2		3,430	top	2392	1993	2748	diatom mud and ooze	Domack & alii, 1999
NBP95-01	kasten core	KC37	-74.498	167.743	924	175	40-41	AIOM	8,630	AA-17359	85	na	5,855	5,855	top	5,400	4,963	5,782	ash-rich sand	Cunningham & alii, 1999
NBP95-01	kasten core	KC37	-74.498	167.743	924	175	40-41	AIOM	8,630	AA-17359	85	-26.8		5,850	top	5400	4963	5782	diatom mud and ooze	Domack & alii, 1999
NBP95-01	kasten core	KC37	-74.498	167.743	924	175	55-56	AIOM	10,495	AA-17361	75	na	7,720	7,720	top	7,411	7,070	7,735	ash-rich sand	Cunningham & alii, 1999
NBP95-01	kasten core	KC37	-74.498	167.743	924	175	55-56	AIOM	10,500	AA-17361	75	-27.7		7,720	top	7411	7070	7735	sandy diatom mud	Domack & alii, 1999
NBP95-01	kasten core	KC37	-74.498	167.743	924	175	67-68	AIOM	13,835	AA-17360	95	na	11,060	11,060	top	11,511	11,052	12,060	massive mud	Cunningham & alii, 1999
NBP95-01	kasten core	KC37	-74.498	167.743	924	175	67-68	AIOM	13,840	AA-17360	95	-26.6	12,930	11,060	top	11,511	11,052	12,060	silty clay	Domack & alii, 1999
NBP95-01	kasten core	KC37	-74.498	167.743	924	175	83-84	AIOM	17,800	AA-20747	175	na	15,025	15,025	top	16,612	16,016	17,191	massive mud	Cunningham & alii, 1999
NBP95-01	kasten core	KC37	-74.498	167.743	924	175	93-95	AIOM	19,385	AA-23228	135	na	16,610	16,610	top	18,480	18,046	18,913	massive mud	Cunningham & alii, 1999
NBP95-01	kasten core	KC37	-74.498	167.743	924	175	146-148	AIOM	26,895	AA-20748	375	na	24,120	24,120	top	26,861	26,036	27,616	pebbly. massive diamicton	Cunningham & alii, 1999
NBP95-01	kasten core	KC39	-74.473	173.512	557	275	top	AIOM	1,270	na_22		na	70	modern	top	#N/D	#N/D	#N/D	mud	Licht & alii, 1996
NBP95-01	kasten core	KC39	-74.473	173.512	557	275	0-1	AIOM	3,140	AA-17351	50	na	0	0	top	0	0	0	massive mud	Cunningham & alii, 1999
NBP95-01	kasten core	KC39	-74.473	173.512	557	275	0-1	AIOM	3,140	AA-17351	50	-28.3		0	top	0	0	0	diatom mud and ooze	Domack & alii, 1999
NBP95-01	kasten core	KC39	-74.473	173.512	557	275	50-51	AIOM	4,755	AA-17355	60	na	1,615	1,615	top	440	123	718	massive mud	Cunningham & alii, 1999
NBP95-01	kasten core	KC39	-74.473	173.512	557	275	50-51	AIOM	4,760	AA-17355	60	-28.9		1,620	top	440	123	718	diatom mud and ooze	Domack & alii, 1999
NBP95-01	kasten core	KC39	-74.473	173.512	557	275	80-82	AIOM	5,820	AA-21770	90	na	2,680	2,680	top	1,486	1,117	1,883	massive mud	Cunningham & alii, 1999
NBP95-01	kasten core	KC39	-74.473	173.512	557	275	100-101	AIOM	7,015	AA-17353	60	na	3,875	3,875	top	2,933	2,553	3,331	massive mud	Cunningham & alii, 1999
NBP95-01	kasten core	KC39	-74.473	173.512	557	275	100-101	AIOM	7,020	AA-17353	60	-28.2		3,880	top	2933	2553	3331	diatom mud and ooze	Domack & alii, 1999
NBP95-01	kasten core	KC39	-74.473	173.512	557	275	150-151	AIOM	7,740	AA-17356	60	na	4,600	4,600	top	3,821	3,419	4,238	massive mud	Cunningham & alii, 1999
NBP95-01	kasten core	KC39	-74.473	173.512	557	275	150-151	AIOM	7,740	AA-17356	60	-28.4		4,600	top	3821	3419	4238	diatom mud and ooze	Domack & alii, 1999
NBP95-01	kasten core	KC39	-74.473	173.512	557	275	170-172	AIOM	8,980	AA-21771	70	na	5,840	5,840	top	5,390	4,966	5,750	massive mud	Cunningham & alii, 1999
NBP95-01	kasten core	KC39	-74.473	173.512	557	275	190-191	AIOM	10,445	AA-17354	80	na	7,305	7,305	top	6,990	6,613	7,349	massive mud	Cunningham & alii, 1999
NBP95-01	kasten core	KC39	-74.473	173.512	557	275	190-192	AIOM	10,450	AA-17354	80	-28.5		7,310	top	6990	6613	7349	silt clay	Domack & alii, 1999
NBP95-01	kasten core	KC39	-74.473	173.512	557	275	208-210	AIOM	14,290	AA-17352	95	na	11,150	11,150	top	11,636	11,157	12,191	sandy mud	Cunningham & alii, 1999
NBP95-01	kasten core	KC39	-74.473	173.512	557	275	208-210	AIOM	14,290	AA-17352	95	-26.7	13,010	11,150	top	11,636	11,157	12,191	muddy gravel	Domack & alii, 1999
NBP95-01	kasten core	KC39	-74.473	173.512	557	275	249-250	AIOM	25,750	AA-19925	320	na	22,610	22,610	top	25,363	24,547	26,047	pebbly. massive diamicton	Cunningham & alii, 1999
NBP95-01	kasten core	KC39	-74.473	173.512	557	275	230	AIOM	26,585	AA-19924	280	na	23,445	23,445	top	26,213	25,624	26,933	pebbly. massive diamicton	Cunningham & alii, 1999
NBP95-01	piston core	PC49	-73.000	171.743	607	98	90-91	AIOM	4,480	AA-19488	120	-26.3		1,480	3 ka	323	1	598	na	Domack & alii, 1999
NBP95-01	piston core	PC49	-73.000	171.743	607	98	65-66	AIOM	5,280	AA-19489	75	-26.8		2,280	3 ka	1,063	717	1,381	na	Domack & alii, 1999
NBP95-01	trigger (gravity) core	TC40	-74.473	173.507	556	45	0-2	AIOM	4,170	AA-19483	65	-27.9		0	top	0	0	0	na	Domack & alii, 1999
NBP95-01	trigger (gravity) core	TC40	-74.473	173.507	556	45	24-26	AIOM	4,540	AA-19484	65	-28.4		370	top	#N/D	#N/D	#N/D	na	Domack & alii, 1999
NBP95-01	trigger (gravity) core	TC40	-74.473	173.507	556	45	43-45	AIOM	5,420	AA-19485	70	-27.5		1,250	top	#N/D	#N/D	#N/D	na	Domack & alii, 1999
TR17	piston core	05PC	-74.299	166.799	777	344	0-1	AIOM	3,620	AWI-4823.1.2	20	-26	600	0	top	0	0	0	diatomaceous ooze	Di Roberto & alii, 2020
TR17	piston core	05PC	-74.299	166.799	777	344	62-63	AIOM	7,850	Poz-111_982	50	na	5610	4,230	top	3357	2956	3746	diatomaceous ooze	Di Roberto & alii, 2020
TR17	piston core	05PC	-74.299	166.799	777	344	98-99	AIOM	17,514	AWI-4824.1.2	240	-18.7	17660	13,894	top	15114	14206	15892	diatomaceous ooze	Di Roberto & alii, 2020
TR17	piston core	12PC	-74.147	166.089	912	450	0-1	AIOM	2,093	AWI-4825.1.1	37	-21.3	modern	0	top	0	0	0	diatomaceous ooze	Di Roberto & alii, 2020
TR17	piston core	12PC	-74.147	166.089	912	450	397-398	AIOM	9,000	Poz-111_979	50	na	7,590	6,907	top	6,547	6,210	6,902	diatomaceous ooze	Di Roberto & alii, 2020
TH95	gravity core	GCI604	-74.550	168.000	922	254	na	na	na	na	na	na	9500	-	-	#N/D	#N/D	#N/D	na	Yokoyama & alii, 2016

## REFERENCES

- ANDREWS J.T., DOMACK E.W., CUNNINGHAM W.L., LEVENTER A., LICHT K.J., TIMOTHY JULL A.J., DEMASTER D.J. & JENNINGS A.E. (1999) - *Problems and Possible Solutions Concerning Radiocarbon Dating of Surface Marine Sediments, Ross Sea, Antarctica*. Quaternary Research, 52 (2), 206-216. doi: 10.1006/qres.1999.2047
- BRAMBATI A., FANZUTTI G.P., FINOCCHIARO F., MELIS R., FRIGNANI M., RAVAIOLI M. & SETTI M. (1997) - *Paleoenvironmental record in Core ANTA91-30 (Drygalski Basin, Ross Sea, Antarctica)*. In: COOPER A.K., BARKER P.F. & BRANCOLINI G. (Eds.), *Geology and Seismic Stratigraphy of the Antarctic Margin. Part 2*. Antarctic Research Series, 71, 137-151.
- BRAMBATI A., MELIS R., QUAIÀ T. & SALVI G. (2002) - *Late Quaternary climatic changes in the Ross Sea area, Antarctica*. In: GAMBLE, J.A., SKINNER, D.N.B. & HENRYS, S. (Eds), *Antarctica at the close of the millennium*. Royal Society New Zealand Bulletin, 35, 359-364.
- COLIZZA E., FINOCCHIARO F., MARINONI L., MENEGAZZO VITTURI L. & BRAMBATI A. (2003) - *Tephra Evidence in Marine Sediments from the Shelf of the Western Ross Sea*. Terra Antarctica, 8, 121-126.
- COLIZZA E., FINOCCHIARO F., IVALDI R. & TOLOTTI R. (2004) - *Sedimentazione fine della Wood Bay (Mare di Ross Occidentale, Antartide)*. Atti dell'Associazione Italiana di Oceanologia e Limnologia 17, 137-148. <http://hdl.handle.net/11368/1746862>
- CUNNINGHAM W.L., LEVENTER A., ANDREWS J.T., JENNINGS A.E. & LICHT K.J. (1999) - *Late Pleistocene-Holocene marine conditions in the Ross Sea, Antarctica: evidence from the diatom record*. The Holocene, 9 (2), 129-139. doi: 10.1191/095968399675624796
- DI ROBERTO A., ALBERT P.G., COLIZZA E., DEL CARLO P., DI VINCENZO G., GALLERANI A., GIGLIO F., KUHN G., MACRÌ P., MANNING C.J., MELIS R., ROCCHI S., SCATENI B., SMITH V.C., TORRICELLA F. & WINKLER A. (2020) - *Evidence for a large-magnitude Holocene eruption of Mount Rittmann (Antarctica): A volcanological reconstruction using the marine tephra record*. Quaternary Science Reviews, 250, 1-21. doi: 10.1016/j.quascirev.2020.106629
- DOMACK E.W., JACOBSON E.A., SHIPP S. & ANDERSON J.B. (1999) - *Late Pleistocene-Holocene retreat of the West Antarctic Ice-Sheet system in the Ross Sea: Part 2 - Sedimentologic and stratigraphic signature*. The Geological Society of America, 111 (10), 1517-1536. doi: 10.1130/0016-7606(1999)111%3C1517:LPHROT%3E2.3.CO;2
- FINOCCHIARO F., BARONI C., COLIZZA E. & IVALDI R. (2007) - *Pre-LGM open-water conditions south of the Drygalski Ice Tongue, Ross Sea, Antarctica*. Antarctic Science, 19 (3), 373-377. doi: 10.1017/S0954102007000430
- FINOCCHIARO F., MELIS R. & TOSATO M. (2000) - *Late Quaternary environmental events in two cores from Southern Joides Basin (Ross Sea, Antarctica)*. Terra Antarctica Reports, 4, 125-130.
- FRIGNANI M., GIGLIO F., LANGONE L., RAVAIOLI M. & MANGINI A. (1998) - *Late-Pleistocene-Holocene sedimentary fluxes of organic carbon and biogenic silica in the northwestern Ross Sea, Antarctica*. Annals of Glaciology, 27, 697-703.
- HALBERSTADT A.R.W., SIMKINS L.M., ANDERSON J.B., PROTHRO L.O. & BART P.J. (2018) - *Characteristics of the deforming bed: till properties on the deglaciated Antarctic continental shelf*. Journal of Glaciology, 64 (248), 1014-1027. doi: 10.1017/jog.2018.92
- LICHT K.J., JENNINGS A.E., ANDREWS J.T. & WILLIAMS K.M. (1996) - *Chronology of late Wisconsin ice retreat from the western Ross Sea, Antarctica*. Geology, 24 (3), 223-226. doi: 10.1130/0091-7613(1996)024<0223:COLWIR>2.3.CO;2
- MELIS R., COLIZZA E., PIZZOLATO F. & ROSSO A. (2002) - *Preliminary study of the calcareous taphocoenoses in Late Quaternary glacial marine sequences of the Ross Sea (Antarctica)*. Geobios, 35, 207-218. doi: 10.1016/S0016-6995(02)00060-8
- MELIS R. & SALVI G. (2009) - *Late Quaternary foraminiferal assemblages from western Ross Sea (Antarctica) in relation to the main glacial and marine lithofacies*. Marine Micropaleontology, 70 (1-2), 39-53. doi: 10.1016/j.marmicro.2008.10.003
- MEZGEC K., STENNI B., CROSTA X., MASSON-DELMOTTE V., BARONI C., BRAIDA M., CIARDINI V., COLIZZA E., MELIS R., SALVATORE M.C., SEVERI M., SCARCHILLI C., TRAVERSI R., UDISTI R. & FREZZOTTI M. (2017) - *Holocene sea ice variability driven by wind and polynya efficiency in the Ross Sea*. Nature Communications, 8 (1334), 1-12. doi: 10.1038/s41467-017-01455-x
- SALVI C., SALVI G., STENNI B. & BRAMBATI A. (2004) - *Palaeoproductivity in the Ross Sea, Antarctica, during the last 15 kyr BP and its link with ice-core temperature proxies*. Annals of Glaciology, 39, 445-451. doi: 10.3189/172756404781814582
- TAVIANI M., REID D.E. & ANDERSON J.B. (1993) - *Skeletal and isotopic composition and paleoclimatic significance of Late Pleistocene carbonates, Ross Sea, Antarctica*. Journal of Sedimentary Research, 63 (1), 84-90.
- YOKOYAMA Y., ANDERSON J.B., YAMANE M. & OHROUCHI N. (2016) - *Widespread collapse of the Ross Ice Shelf during the late Holocene*. Earth, Atmospheric and Planetary Sciences, 113 (9), 2354-2359. doi: 10.1073/pnas.1516908113

TABLE S4 - Seismic discontinuities and units detected in this study in the Drygalski trough basin. Correspondence to age model at DSDP 273 and to seismic units interpreted in previous studies in the western Ross Sea. CB = Central Basin; NB = Northern Basin; NVL = Northern Victoria Land; SVL = Southern Victoria Land; WB = Wood Bay; LNB = Lady Newnes Bay; RS = Ross Sea; MMS = McMurdo Sound; RI = Ross Island; DB = Drygalski Basin; RSU = Ross Sea Unconformity; RSS = Ross Sea Unit.

References									
Cooper & <i>alii</i> , 1987	DSDP 273 Savage & Ciesielski, 1983	Anderson & Bartek, 1992	Brancolini & <i>alii</i> , 1995a, b, c	Bartek & <i>alii</i> , 1996	Bart & <i>alii</i> , 2000; 2011	Horgan & <i>alii</i> , 2005	Fielding & <i>alii</i> , 2008; Levy & <i>alii</i> , 2012	Sauli & <i>alii</i> , 2014	This study
VLB	CB	Ross Sea	NVL, SVL, NB	MMS	NB edge continental shelf and upper slope	RI	MMS	WB and LNB	DB
V1	Unit 1		RSS8	A/B	Units 1-2 (0.71 Ma to present)	Surface A0	Rk	Unit 2	LGM unconformity
V1	Hiatus (14.7 - 4.0 Ma)	3/2?	RSU1	C/D?	Units 9-3 (2.08-0.71 Ma)	Surface A1	Rj	T	
		5/6	RSU2	E/F	Unconformity 10 (4 Ma?)	Surface A2	Ri-Rv	B	Purple unconformity
			RSS6		Unit 10				
			RSS5	G/H					
V1	Unit 2		RSU4						
			RSS4 (19-16 Ma)						
		9/10	RSU4a			Surface B	Rh		
V2			RSS3						
		10/11	RSU5	L/M		Surface C	Rg		
V3			RSS2						
V3			RSU6	P/Q			Rf		
V3			RSS1	R/S					
							Re		
V4							Rd		
V5				T					
							Rc		
							Rb		
							Ra		
V6				volcanics					
V7				basement					

seismic unit(s) and discontinuity(ies)

## REFERENCES

- ANDERSON J.B. & BARTEK L.R. (1992) - *Cenozoic glacial history of the Ross Sea revealed by intermediate resolution seismic reflection data combined with drill site information*. In: KENNETT J.P. & WARNKE D.A. (Eds.), *The Antarctic paleoenvironment: A perspective on global change*. American Geophysical Union, Antarctic Research Series, 56, 231-263.
- BART P.J., ANDERSON J.B., TRINCARDI F. & SHIPP S.S. (2000) - *Seismic data from the Northern basin, Ross Sea, record extreme expansions of the East Antarctic Ice Sheet during the late Neogene*. *Marine Geology*, 166, 31-50. doi: 10.1016/S0025-3227(00)00006-2
- BART P.J., SJUNNESKOG C. & CHOW J.M. (2011) - *Piston-core based biostratigraphic constraints on Pleistocene oscillations of the West Antarctic Ice Sheet in western Ross Sea between North Basin and AND-1B drill site*. *Marine Geology*, 289 (1-4), 86-99. doi: 10.1016/j.margeo.2011.09.005
- BARTEK L.R., HENRYS S.A., ANDERSON J.B. & BARRETT P.J. (1996) - *Seismic stratigraphy of McMurdo Sound, Antarctica: implications for glacially influenced early Cenozoic eustatic change?* *Marine Geology* 130 (1-2), 79-98. [https://doi.org/10.1016/0025-3227\(95\)00121-2](https://doi.org/10.1016/0025-3227(95)00121-2)
- BRANCOLINI G., COOPER A.K. & COREN, F. (1995a) - *Seismic Facies and Glacial History in the Western Ross Sea, (Antarctica)*. In: COOPER A.K., BARKER P.F. & BRANCOLINI G. (Eds.), *Geology and Seismic Stratigraphy of the Antarctic Margin*. American Geophysical Union, Antarctic Research Series, 68, 209-233. doi: 10.1029/AR068p0209
- BRANCOLINI G., Busetti M., COREN F., DE CILLIA C., MARCHETTI A., DE SANTIS L., ZANOLLA C., COOPER, A.K., COCHRANE G.R., ZAYATZ I., BELYAEV V., KNYAZEV M., VINNIKOVSKAYA O., DAVEY F.J. & HINZ K. (1995b) - *ANTOSTRAT project, seismic stratigraphic atlas of the Ross Sea, Antarctica*. In: COOPER A.K., BARKER P.F. & BRANCOLINI G. (Eds.), *Geology and Seismic Stratigraphy of the Antarctic Margin*. American Geophysical Union, Antarctic Research Series, 68. doi:10.1029/AR068
- BRANCOLINI G., Busetti M., MARCHETTI A., DE SANTIS L., ZANOLLA C., COOPER A.K., COCHRANE, G.R., ZAYATZ I., BELYAEV V., KNYAZEV M., VINNIKOVSKAYA O., DAVEY F.J. & HINZ K. (1995c) - *Descriptive Text for the Seismic Stratigraphic Atlas of the Ross Sea, Antarctica*. In: COOPER A.K., BARKER P.F. & BRANCOLINI G. (Eds.), *Geology and Seismic Stratigraphy of the Antarctic Margin*. American Geophysical Union, Antarctic Research Series, 68, A271-A286. doi: 10.1002/9781118669013.app1
- COOPER A.K., DAVEY F.J. & BEHRENDT J.C. (1987) - *Seismic stratigraphy and structure of the Victoria Land basin, Western Ross Sea, Antarctica*. In: COOPER A.K. & DAVEY F.J. (Eds.), *The Antarctic continental margin, Geology and Geophysics of the Western Ross Sea*. Circum-Pacific Council for Energy and mineral resources, Earth Science Series.
- FIELDING C.R., WHITTAKER J., HENRYS S.A., WILSON T.J. & NAISH T.R. (2008) - *Seismic facies and stratigraphy of the Cenozoic succession in McMurdo Sound, Antarctica: Implications for tectonic, climatic and glacial history*. *Palaeogeography, Palaeoclimatology, Palaeoecology*, 260, 8-29. doi: 10.1016/j.palaeo.2007.08.016
- HORGAN H., NAISH T., BANNISTER S., BALFOUR N. & WILSON G. (2005) - *Seismic stratigraphy of the Plio-Pleistocene Ross Island flexural moat-fill: a prognosis for ANDRILL Program drilling beneath McMurdo-Ross Ice Shelf*. *Global and Planetary Change* 45 (1-3), 83-97. <https://doi.org/10.1016/j.gloplacha.2004.09.014>
- LEVY R., CODY R., CRAMPTON J., FIELDING C., GOLLEDGE N., HARDWOOD D., HENRYS S., MCKAY R., NAISH T., CHRISTIAN O., WILSON G., WILSON T. & WINTER D. (2012) - *Late Neogene climate and glacial history of the Southern Victoria Land coast from integrated drill core, seismic and outcrop data*. *Global and Planetary Change*, 96-97, 157-180. doi: 10.1016/j.gloplacha.2012.02.005
- SAULI C., Busetti M., DE SANTIS L. & WARDELL N. (2014) - *Late Neogene geomorphological and glacial reconstruction of the northern Victoria Land coast, western Ross Sea (Antarctica)*. *Marine Geology*, 355, 297-309. doi: 10.1016/j.margeo.2014.06.008
- SAVAGE M.L. & CIESIELSKI P.F. (1983) - *A revised history of glacial sedimentation in the Ross Sea region*. *Antarctic Earth Science*, 555-559.